Available online at www.sciencedirect.com
SCIENCE DIRECT®
International Journal of Heat and Mass Transfer 47 (2004) 329–340
International Journal of HEAT and MASS TRANSFER
www.elsevier.com/locate/ijhmt

Continuously distributed sensors for steady-state temperature profile measurements: main principles and numerical algorithm

Yu.K. Evdokimov [a], S. Martemianov [b,*]

[a] Kazan State Technical University named after A.N. Tupolev, K. Marx Str. 10, 420111 Kazan, Russia
[b] Laboratory of Heat Studies—LET UMR CNRS 6608, ESIP, University of Poitiers, 40 Avenue du Recteur Pineau, 86022 Poitiers Cedex, France

Received 30 May 2002; received in revised form 10 June 2003

Abstract

Principally new method for measurements of steady-state temperature field is suggested. This method is based on the use of so-called continuously distributed sensors (CDS). The basic CDS function is the measurement of temperature profile along the sensor length.

The CDS can be manufactured my means of microfilm technologies in the form of a rod, flexible thread, or thin film. Only three electrical cables are needed for connection of CDS and measuring equipment. Nevertheless, it is possible to obtain simultaneously the information about temperature profile at several tens space points along the CDS. So, the CDS is equivalent to several tens of conventional discrete sensors, for example, thermocouples.

The measuring process with the use of CDS can be described by the following scheme. A temperature field acts on the CDS causing space non-homogeneity of the electrical parameters of thermo-sensitive films. The space distribution of electrical parameters along CDS can be measured by means of electrical signals of different frequencies. Indeed, the distance to which the electrical signal penetrates the sensor depends on the frequency. So, the measuring impedance of the sensor contains information about space distribution of electrical parameters, which are directly related with the temperature profile.

Restoration of the space distribution of electrical parameters from frequency characteristics of the measuring impedance is non-trivial task. From the mathematical point of view it is inverse problem. Some algorithms for solving of this inverse problem are developed and are presented in the paper. Numerical simulations demonstrate possibilities to measure temperature fields by means of CDS.

1. Introduction

All the now-existing conventional sensors (thermocouples, thermoresistors, ...) make it possible to measure only the local, that is, point characteristics of thermophysical fields. When measuring the spatial structure of these fields, it is necessary to make use of a set of "discrete sensors" installed in the object. Conventional methods lead to a significant sophistication of measuring equipment and to large material expenditures. Indeed a large number of sensors require a corresponding number of measuring channels and very important length of cables (tens and hundreds meters) for connection of sensors and measuring equipment. Another problem is the assembly and maintenance of the measuring system.

A principally new approach to the problem is related with the continuously distributed sensors (CDS). The main principles of CDS are presented in this article. The basic CDS function is the measurement of steady-state temperature field along the sensor length. Information

* Corresponding author.
E-mail addresses: evdokimov@tre.kstu-kai.ru (Yu.K. Evdokimov), martemianov@esip.univ-poitiers.fr (S. Martemianov).

0017-9310/$ - see front matter © 2003 Elsevier Ltd. All rights reserved.
doi:10.1016/j.ijheatmasstransfer.2003.06.002

Nomenclature

C	electrical capacitance per unit length ($\mathrm{F\,m^{-1}}$)
C_0	electrical capacitance per unit length at $T = T_0$ ($\mathrm{F\,m^{-1}}$)
G	Green function
I	complex amplitude of current at the arbitrary point x
I_S	complex amplitude of input current at $x = 0$
j	imaginary unit $= \sqrt{-1}$
k_R, k_C	temperature sensitivity coefficients of longitudinal resistance and capacitance ($\Omega\,\mathrm{m^{-1}\,K^{-1}}$, $\mathrm{F\,m^{-1}\,K^{-1}}$)
l	length of the sensor
l_x	effective distance of penetration of the sounding signal
Δl	spatial step of the measurement
m	total number of elementary links in CDS electrical model
n	number of iterations
N	number of discrete sensors
N_x	number of steps on the numerical grid in space domain
N_ω	number of steps on the numerical grid in frequency domain
p	complex frequency $= \mathrm{j}\omega$, ($\mathrm{rad\,s^{-1}}$)
R	longitudinal resistance of the sensor per unit length ($\Omega\,\mathrm{m^{-1}}$)
R_0	longitudinal resistance of the sensor per unit length at $T = T_0$ ($\Omega\,\mathrm{m^{-1}}$)
ΔR	variation of longitudinal resistance
T	temperature
T_0	temperature of the uniform field
ΔT	temperature variation
U	complex amplitude of voltage at the arbitrary point x
U_S	complex amplitude of the input voltage at $x = 0$
x	longitudinal coordinate along the sensor
Δx	spatial step $= l/(N_x - 1)$
Y	admittance at the arbitrary point x along the sensor length (S)
Y_l	admittance of the external load at the right end of the sensor (S)
Y_S	measuring admittance of the sensor, corresponds to the admittance at $x = 0$ (S)
y_0	cross conductivity per unit length ($\mathrm{S\,m^{-1}}$)
Δy_0	variation of cross conduction ($\mathrm{S\,m^{-1}}$)
y_r	cross conductivity of non-ideal dielectric material per unit length (leakage $y_r = 1/r_y$ conductivity) ($\mathrm{S\,m^{-1}}$)
Z	impedance at the arbitrary point x along the sensor length (Ω)
Z_S	measuring impedance of the sensor, corresponds to the impedance at $x = 0$ (Ω)

Dimensionless group

$\overline{R}$	longitudinal resistance, R/R_0
$\overline{T}$	temperature, T/T_0
$\bar{x}$	longitudinal coordinate along the sensor, x/l
$\overline{Y}$	input admittance, YR_0l
$\bar{y}_0$	cross conductivity, $y_0R_0l^2$
$\bar{\omega}$	frequency, $\omega R_0C_0\Delta x^2$

Greek symbols

α_T	regularization parameter
δ	small perturbation or variation
ε_R	error of the right-hand side of the Fredholm's equation
ε_S	mean-square measuring error
ε_{max}	maximum error of the restoration
ε_{res}	mean-square error of the restoration
ω	frequency ($\mathrm{rad\,s^{-1}}$)
ω_{max}	maximum frequency
ω_{min}	minimum frequency
$\Delta\omega$	frequency step

which can be obtained by means of the CDS is equivalent to several tens of conventional discrete sensors. Furthermore, CDS extend significantly the scope of the thermophysical measurements.

The CDS can be manufactured in the form of a rod, flexible thread, or thin film. The employment of modern microfilm technologies makes it possible to realize CDS on the basis of distributed electrical resistive–capacitive (RC) filmy structures, distributed semiconducting diode structures [1] and also distributed electrochemical structures [2–4]. For connecting of CDS with measuring equipment only three cables are needed. So, it is possible to simplify significantly the assembly and maintenance of measuring systems. Another important advantage is the decreasing of a number of measuring channels. In principle, for CDS only one measuring channel is needed.

A simplicity of the measuring system on the basis of CDS is achieved by use rather sophisticated data treatment. The development of the appropriative algorithms of data treatment for CDS is the main goal of the paper. The measuring process with the use of CDS can be described by the following scheme. Temperature field acts on the CDS causing space non-homogeneity of the electrical parameters of thermo-sensitive films. The space distribution of these parameters along CDS can

be measured by means of electrical signals of different frequencies. Indeed, the distance to which the electrical signal penetrates the sensor depends on its frequency. So, the measuring impedance of the sensor contains information about space distribution of the electrical parameters which are directly related with the temperature profile.

Restoration of the space distribution of the electrical parameters from frequency characteristics of the measuring impedance is non-trivial task. From the mathematical point of view it is inverse problem [5,6]. The computational capabilities of the present-day computers allow realizing rather sophisticated algorithms in real time. In this way we have developed some numerical procedures which demonstrate possibilities to measure temperature field distribution by means of CDS.

2. Principles of CDS design

To simplify the presentation of CDS principles we consider as an example the case of measurements of one-dimensional temperature field $T(x)$ at the surface of solid bodies. Usually the temperature at the solid surfaces is measured with the aid of contact sensors of temperature, for example, thermocouples or thermo resistors. For measurements of the temperature profile $T(x)$ a set of "discrete" temperature sensors is used.

Let us suppose that for measurements of the temperature field N sensors should be placed with a given spatial step Δl at the surface of the body (Fig. 1(a) and (b)). All sensors have a pair of the electric wires. To connect the sensors electrically to the secondary electronic equipment, it is necessary to have $2N$ wires of corresponding length. If $N = 30$ and the average distance from sensors to the measuring system is 10 m, it is necessary to use 30 amplifying electronic units and approximately $2N \cdot 10 = 600$ m of cables. It might be well to note the high cost of the measuring system with N amplifiers, and also the high cost of wiring and system maintenance. Moreover, the heat leakage along $2N$ wires can distort significantly the temperature measured. This problem becomes very important for microsystems.

In this paper a new method for temperature field measurements is proposed. The method is based on use of the so-called "CDS" (Fig. 1(c)) that is equivalent to N conventional "discrete" sensors (Fig. 1(b)). There are two possibilities for connection of CDS and measuring equipment (Fig. 2). When CDS is connected from one of its ends, only two cables are required. For the connection from both ends ($x = 0, x = l$), three cables are needed.

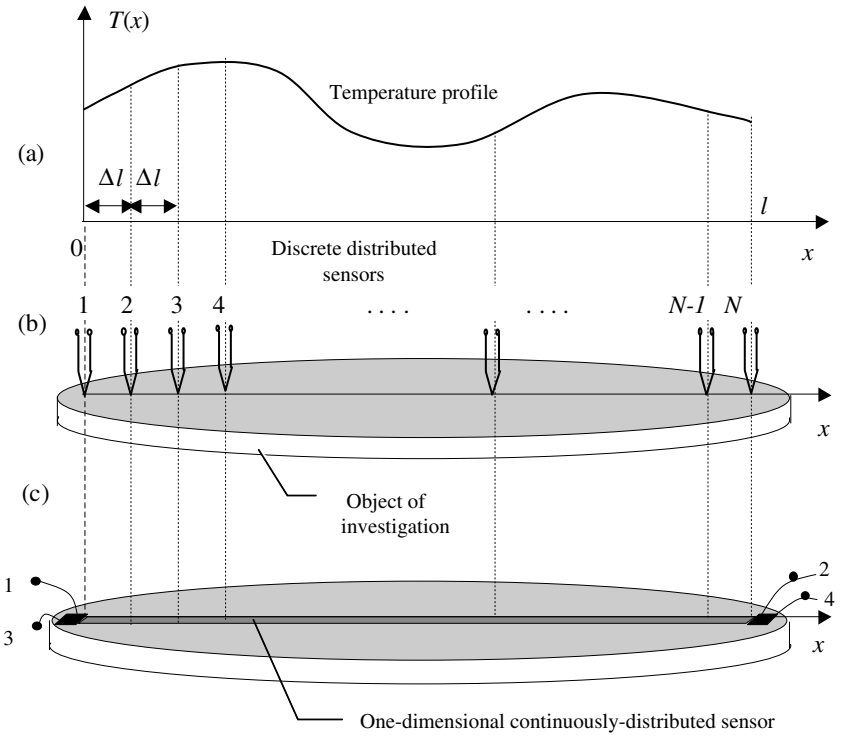

Fig. 1. Temperature field measurements: (a) temperature profile; (b) conventional discretely distributed sensors, for example, thermocouples; (c) one-dimensional CDS.

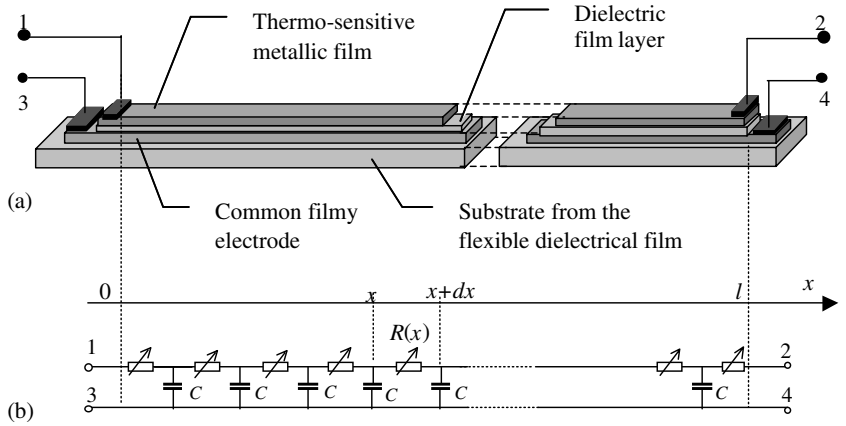

Fig. 2. Design of one-dimensional CDS on the basis of microfilm technologies: (a) multi-layers microfilm structures; (b) equivalent electrical model of CDS.

In this paper only one possible type of CDS will be considered. This sensor can be fabricated on the basis of modern microfilm technologies as a multi-layers RC structure. Concrete design of the thin-film three-layers structure is presented in Fig. 2. The sensor is formed by the upper resistive thermo-sensitive film, by the middle layer of dielectric, and by the lower metallic film that plays the role of a common electrode. As the support for this three-layers structure a flexible polymeric film can be used.

The upper thermo-sensitive layer has two electrical outputs 1,2 for external electrical connections. The lower layer has two outputs 3,4 which are completely equivalent from the electrical point of view (common electrode).

In the real sensor, the thickness of metallic and dielectric films as well as the thickness of the support is very small (about 0.1–10 μm). As a result, thermal resistance of the sensor in the normal direction is significantly smaller as compared with the thermal resistance in the longitudinal direction. That is why we assume that the temperature distribution along the sensor is identical to the temperature profile $T(x)$ of the examined object.

The measuring process can be described by the following scheme. The temperature field $T(x)$ acts on the CDS causing a variation of the electrical resistance $R(x)$ of the upper thermo-sensitive film. Let the film sensitivity to the temperature be known:

$$\Delta R = k_R \Delta T, \quad R = R_0(1 + k_R \Delta T), \tag{1}$$

where k_R is the temperature coefficient of the sensitive film, R_0 is the electrical resistance of the film at $T = T_0$ and $\Delta T = T - T_0$. We note that R and R_0 are the electrical resistances per unit length.

In view of Eq. (1), the distribution of the electrical resistance $R(x)$ of the thermo-sensitive film will then be similar to that of the temperature profile:

$$R(x) = R_0 + \Delta R(x) = R_0[1 + k_R \Delta T(x)], \quad 0 \leqslant x \leqslant l. \tag{2}$$

The space distribution of the electrical parameters along CDS can be measured by means of electrical signals of different frequencies. To simplify the presentation, we consider below the case when the sensor is connected from the one end ($x = 0$). Let us suppose that we apply a sinusoidal voltage between connections 1 and 3 (see Fig. 2) and measure the electrical current. In other words, we measure the electrical impedance $Z_S(j\omega)$ of the sensor in the frequency range $\omega_{min} \leqslant \omega \leqslant \omega_{max}$:

$$x = 0: \quad Z_S(j\omega) = Z_{13}(j\omega) = U_S(j\omega)/I_S(j\omega), \tag{3}$$

where $U_S(j\omega)$ and $I_S(j\omega)$ are the complex amplitudes of the input voltage and current.

The temperature profile $T(x)$ can be found, in accordance with Eq. (2), if we know a distribution of the electrical resistance $R(x)$ along the sensor length $0 \leqslant x \leqslant l$. The distribution of $R(x)$ can be restored from of the measured impedance $Z_S(j\omega)$. This is the inverse problem which is related to the class of ill-posed Hadamard problems [6,7]. Algorithms for solving the above-posed inverse problem form the basis of the measuring procedure with the use of CDS.

The physical sense of the proposed method is as follows. The distance l_x, to which the electrical signal $U_S(j\omega)$ penetrates from the left end of the sensor ($x = 0$) depends on its frequency ω and the electrical parameters of the films R and C, where C is the electrical capacitance of the three-layers structure per unit length. The effective distance of penetration is proportional to $l_x \sim (\omega RC)^{-1/2}$ and increases as the frequency decreases. Thus, it is possible to restore $R(x)$ distribution by using $Z_S(j\omega)$ data and by solving the inverse problem. The concrete algorithms of solving the inverse problem are discussed in the next paragraphs.

3. Mathematical model of CDS

Fig. 3(b) presents the generalized electrical model of CDS in the form of cascade connection of elementary components. The infinitesimal section of the sensor, dx, is modeled by longitudinal resistance of the upper thermo-sensitive film $R(x)$ and by the cross conductivity $y_0(x,p)$, where $p = j\omega$ is the complex frequency. The cross conductivity y_0 is presented as a sum of the electrical capacitance of the dielectric material, pC, and the conductivity of a leakage, $y_r = 1/r_y$, due to non-ideality of the dielectric material (Fig. 3(c)):

$$y_0(x,p) = pC(x) + y_r(x). \tag{4}$$

The electrical capacitance and the leakage conductivity depend on the temperature. So, the dependence of these parameters on the coordinate x appears in Eq. (4). Small variations of the temperature field $\Delta T(x)$ cause small variations of the cross conductivity $\Delta y_0(x,p)$. As a result:

$$\begin{aligned}\Delta y_0(x,p) &= pk_C\Delta T(x) + k_y\Delta T(x)\\ &= (pk_C + k_y)\Delta T(x).\end{aligned} \tag{5}$$

Coefficient k_C and k_y characterize temperature sensitivity of the electrical capacitance and the leakage conductivity. Fig. 3(a) presents the qualitative example of the temperature field distribution, $T(x)$, and corresponding profiles $R(x)$, $C(x)$, and $r_y(x)$. In the general case, these temperature coefficients may have different signs.

Let us obtain the governing equations for the mathematical model of CDS. The gradient of potential and the gradient of current along the sensor are given by differential Ohm law:

$$-\frac{dU}{dx} = R(x)I; \tag{6}$$

$$-\frac{dI}{dx} = y_0(x,p)U. \tag{7}$$

Replacing the derivative dU/dx in Eq. (6) by means of Eq. (7), we obtain the equation for the current distribution $I(x)$:

$$\frac{d^2I}{dx^2} - \frac{d(\ln y_0)}{dx}\cdot\frac{dI}{dx} - Ry_0I = 0; \tag{8}$$

The dual equation can be obtained for the voltage distribution $U(x)$:

$$\frac{d^2U}{dx^2} - \frac{d(\ln R)}{dx}\cdot\frac{dU}{dx} - Ry_0U = 0; \tag{9}$$

Let us introduce the notions of the electrical impedance $Z(x,p)$ and the admittance $Y(x,p)$ of CDS at the arbitrary point x as (Fig. 3):

$$Z(x,p) = \frac{U(x,p)}{I(x,p)}; \quad Y(x,p) = \frac{1}{Z(x,p)}. \tag{10}$$

For $x = 0$ the impedance $Z(x,p)$ is equal to the measuring impedance of the sensor $Z(0,p) = Z_S(p)$.Taking account Eqs. (7) and (10) the following relations can be obtained:

$$Zy_0 = -\frac{1}{I}\frac{dI}{dx}; \quad \text{and} \quad \frac{1}{I}\frac{d^2I}{dx^2} = (Zy_0)^2 - \frac{d(Zy_0)}{dx}. \tag{11}$$

Replacing the derivatives in Eq. (8) by means of relations (11), we obtain the non-linear differential Riccati's equation for the impedance of CDS:

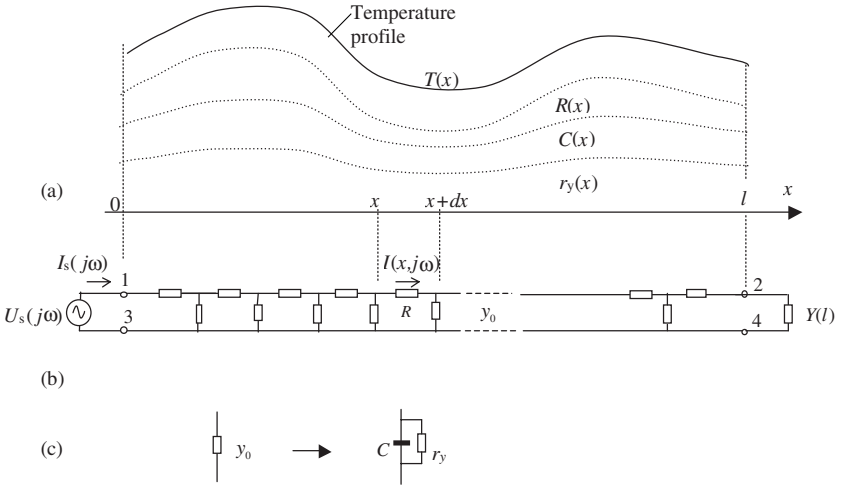

Fig. 3. Generalised electrical model of CDS: (a) temperature profile and corresponding space distributions of the electrical parameters of CDS; (b) scheme of electrical connection of CDS; (c) electrical model of cross conductivity of CDS.

$$\frac{dZ(x,p)}{dx} - y_0(x,p)Z^2(x,p) + R(x) = 0. \quad (12)$$

In the same way it is possible to obtain the Riccati's equation for the admittance of CDS:

$$\frac{dY(x,p)}{dx} - R(x)Y^2(x,p) + y_0(x,p) = 0. \quad (13)$$

Two dual equations (12) and (13) present the mathematical model of CDS.

4. Inverse problem statement. Spectral method

In this section, we formulate the mathematical statement of the inverse problem. The solution of the inverse problem is necessary for restoration of the temperature profile by means of the sensor impedance (or admittance) measurements. Since for the restoration of the temperature profile the frequency signals are used, we shall call this algorithm the spectral method.

The scheme of measurements is presented in Fig. 3. In this scheme the external load Y_l is connected to the right end of the sensor, so:

$$x = l: \quad Y(l,p) = Y_l. \quad (14)$$

Let $Y_S(p)$ be the result of measurements of the CDS admittance obtained from the left end of the sensor:

$$x = 0: \quad Y_S(p) = Y(0,p) = \frac{I_S(0,p)}{U_S(0,p)},$$

$$\omega_{\min} \leqslant \omega \leqslant \omega_{\max}. \quad (15)$$

In this paper the inverse problem is formulated as follows: based on the measurements of $Y_S(p)$, it is required to determine in Eq. (13) either the coefficient $R(x)$ (supposing that $y_0 = \text{cte}$) or the coefficient $y_0(x,p)$ (supposing that $R = \text{cte}$). Hereinafter the space distribution $T(x)$ of the temperature field along the sensor length $0 \leqslant x \leqslant l$ can be obtained from Eqs. (2) and (5).

It must be recalled that the Riccati's equations (12) and (13) are directly related with second-order Sturm–Liouville ordinary differential equations (8) and (9) in the spectral domain. Determining of the distributions $y_0(x,p)$ and $R(x)$ in these equations relates to the class of inverse Sturm–Liouville problems [5,8,9]. These problems have been studied by means of analytical methods but for rather restricted class of functions (see Gel'fand–Levitan method [8]). As examples, we can cite the inverse problem for telegraph equations for ideal lines without losses [10] and the inverse problems on propagation of elastic waves in seismology [11]. In these cases the characteristic wave resistances were the real and positive functions.

The difficulties of generalization of the analytical methods for non-ideal mediums with losses are discussed in [12]. In the case of CDS the losses cannot be omitted and the cross conductivity $y_0(p)$ has a complex structure (see Eq. (4)). This fact forces one to develop numerical methods of solving the inverse problems in spectral domain.

The numerical algorithms for solving the inverse problems in spectral domain are constructed by using preliminary Laplace or Fourier transformations of starting equations [11,13]. The transformed equations are the ordinary second-order differential equations with coefficients that are variable along the coordinate x. These equations can be solved if represented in the form of integral equations. In this way, there were developed [13] the algorithms for restoration of the thermal conductivity in the heat conduction equation. In [11], there was proposed the iterative method of solving the inverse problem for continuously stratified elastic medium with respect to the restoration of the coefficient of seismic wave reflection. In the last paper [11] the non-linear Riccati's equation is used for the coefficient of reflection.

In this paper a spectral algorithm is proposed for solving the inverse problem for CDS. Unlike the well-known algorithms, the herein-presented approach is based on the small perturbations method and the linearization of Riccati's equation. This procedure makes it possible to reduce the original problem to the equivalent integral equation with a simply structured kernel. The solution of the latter equation is introduced in the general iterative procedure. In its formulation, the original inverse problem is ill-posed. That as why, the use of regularization methods is needed [7].

As a rule, electrical properties of thin dielectrical films are very sensitive to the temperature. At the same time, it is possible to fabricate the metallic films with temperature independent electrical resistance. That is why in the following paragraphs we have neglected the temperature dependence of the electrical resistance R in comparison with the electrical conductivity y_0 and have considered R as a constant. Our goal is related with restoration of the cross conductivity y_0 of the sensor by means of impedance (admittance) measurements for the case when $R = \text{cte}$.

5. Iterative algorithm for inverse problem

5.1. Main principles of the algorithm

The main idea of the algorithm is as follows. Small perturbations $\delta y_0(x,p)$ of the cross conductivity $y_0(x,p)$ with respect to the stationary distribution give rise to small variations $\delta Y(x,p)$ of CDS admittance $Y(x,p)$. This fact makes it possible to linearize the original non-linear Riccati's equation (13) with respect to the small

perturbations $\delta Y(x,p)$, $\delta y(x,p)$ and to obtain the corresponding linear first-order differential equation. We obtain then the equivalent Fredholm's first-kind integral equation that couples the perturbations of the sensor admittance $\delta Y_S = \delta Y(0,p)$ with that of the conductivity $\delta y_0(x,p)$. The so-found solution $\delta y_0(x,p)$ of the integral equation is introduced in the form of small corrections into the general iterative procedure

$$y_{0(n+1)} = y_{0n}(x,p) + \delta y_{0n}(x,p),$$

where n is the iteration index. The iterative procedure is continued until the difference between the measured and the calculated admittance of the sensor

$$\delta Y_n = Y_S(p) - Y_n(0,p)$$

attains the prescribed small value.

The perturbation method reduces the original inverse problem to a number of simpler linear problems that can be solved by means of standard computational procedures.

5.2. Integral equation relating perturbations of the sensor admittance and the cross conductivity

Let us consider the iterative process:

$$Y_{n+1}(x,p) = Y_n(x,p) + \delta Y_n(x,p); \tag{16}$$

$$y_{0(n+1)}(x,p) = y_{0n}(x,p) + \delta y_{0n}(x,p), \quad n = 0,1,2,\ldots, \tag{17}$$

where n is the iteration index; δY, δy_0 are small perturbations of the admittance and the cross conductivity of CDS, respectively. Substituting in Eq. (13)

$$Y_n(x,p) + \delta Y_n(x,p);$$

$$y_{0(n+1)}(x,p) = y_{0n}(x,p) + \delta y_{0n}(x,p)$$

and omitting the second-order terms $O(\delta Y_n^2)$, we obtain the non-linear Riccati's equation for Y_n:

$$\frac{dY_n(x,p)}{dx} - RY_n^2(x,p) + y_{0n}(x,p) = 0 \tag{18}$$

and the linear equation for perturbations δY_n

$$\frac{d\delta Y_n(x,p)}{dx} - 2RY_n\delta Y_n(x,p) + \delta y_{0n}(x,p) = 0. \tag{19}$$

The initial conditions on the right end of CDS have the form:

$$x = l: \quad Y_n(l,p) = Y_l; \quad \delta Y_n(l,p) = 0. \tag{20}$$

Let us obtain the integral equation that is equivalent to Eq. (19) and that relates the small perturbations of $\delta y_{0n}(x,p)$ and $\delta Y_n(x,p)$. The solution of Eq. (19) with the initial conditions (20) can be presented in the integral form:

$$\int_x^l G(x,x',p)\delta y_{0n}(x',p)\,dx' = \delta Y_n(x,p), \tag{21}$$

where $p = j\omega$ is a complex frequency. The kernel G of this integral equation is given by the Green function [14]:

$$x < x': \quad G = G(x,x',p) = \exp\left[-2R\int_x^{x'} Y_n\,dx\right]; \tag{22}$$

$$x > x': \quad G = G(x',x,p). \tag{23}$$

Let

$$\delta Y_n(0,p) = Y_S(p) - Y_n(0,p) \tag{24}$$

be the difference between the measured value of the sensor admittance $Y_S(p)$ and its iterative approximation $Y_n(0,p)$. If we take into account Eqs. (22)–(24) the integral equation (21) can be transformed to the form:

$$\int_0^l \exp\left[-2R\int_0^{x'} Y_n\,dx\right]\delta y_{0n}(x',p)\,dx' = Y_S(p) - Y_n(0,p). \tag{25}$$

Eq. (25) is the integral Fredholm's equation of the first kind. Its physical meaning is the following. Local perturbations of the cross conductivity $\delta y_{0n}(x,p)$ at a point x of CDS results in variations of the sensor admittance $\delta Y_S(p)$. The "partial" contribution of the local perturbation $\delta y_{0n}(x,p)$ decreases exponentially in accordance with the Green function (22) when the distance x from the left end of the sensor increases.

It is necessary to take into account that in real applications the right-hand side of Eq. (25) is sensitive to the accuracy of experimental data. As is known, the problem of solving the integral Fredholm's equation of the first kind (25) is ill-posed [7]. That is why some regularization procedures, as for example the Tikhonov's method [7,15] should be used. For solving the first kind Fredholm's equation, there exists a number of highly efficient numerical procedures in the form of standard application programs [15,16] and we have made use of them.

5.3. Data treatment algorithm for CDS

Data treatment algorithm is based on the relations (14)–(18), (20), (24), (25), and includes the following steps:

1. According to Eq. (15), we measure the frequency characteristic of the sensor admittance $Y_S(p)$ of CDS in the frequency range $\omega_{\min} \leqslant \omega \leqslant \omega_{\max}$;
2. We specify the initial approximation for the space distribution of the electrical conductivity $y_{00}(x,p)$;

3. We solve the Riccati's equation (13) with the initial conditions Eq. (20) and we find $Y_n(x,p)$. The details of the solution of the Riccati's equation are presented in Appendix A;
4. We solve the integral Fredholm's equation of the first kind by means of Tikhonov's regularization and we find the distribution $\delta y_{0n}(x,p)$;
5. If the square of the norm $\int_0^l |\delta y_{0n}|^2 \,\mathrm{d}x < \varepsilon_f^2$, where ε_f is the prescribed accuracy, the iterative process is terminated and we pass to the item 6. Otherwise, we find the next approximation $y_{0(n+1)} = y_{0n} + \delta y_{0n}$ and pass to the item 3;
6. Based on the so-found space distribution of the cross conductivity $y_{0m}(x,p)$ and Eq. (5), we calculate the temperature profile $T(x)$ along the sensor.

The above presented algorithm is based on thermal sensitivity of the cross conductivity y_0. If thermal sensitivity of the longitudinal resistance $R(x)$ is used in the measurements the algorithm remains to be valid (for the case of $y_0 = \text{const}$), since Eqs. (12) and (13) are dual. In this case, we must use the Riccati's equation (12) for the impedance $Z(x,p)$, introduce the iterative procedure using the following relations:

$$Z_{n+1}(x,p) = Z_n(x,p) + \delta Z_n(x,p);$$
$$R_{n+1}(x) = R_n + \delta R_n(x) \tag{26}$$

and substitute δy_{0n} and δY_n in other formulas for δR_n and δZ_n, respectively.

6. Numerical simulation of measurements by means of CDS

6.1. Computational procedure

For estimations of measuring possibilities of CDS numerical simulations were used. The physical structure of CDS (Fig. 2(a)) was simulated by the equivalent electrical scheme (Fig. 3(b)). The restoration of the temperature field along CDS was done by using the above-presented data treatment algorithm. Computational procedure was carried out in accordance with the steps 1–6 of this algorithm (see Section 5.3).

By means of the dimensionless variables $\bar{x} = x/l$; $\bar{y}_0 = y_0 R_0 l^2$; $\overline{R} = R/R_0$; $\overline{Y} = YR_0 l$; $\overline{T} = T/T_0$; $\bar{\omega} = \omega R_0 C_0 \Delta x^2$, we can present Eqs. (13) and (14) in the following form:

$$\frac{\mathrm{d}\overline{Y}}{\mathrm{d}\bar{x}} - \overline{R}\overline{Y}^2 + \bar{y}_0 = 0; \quad 0 \leqslant \bar{x} < 1, \tag{27}$$

$$\bar{x} = 1: \quad \overline{Y} = \overline{Y}_1. \tag{28}$$

Here R_0, C_0 are the electrical resistance and capacitance at a given temperature T_0, $\Delta x = l/(N_x - 1)$. In our simulations we have accepted that the admittance of the external load at the right end of the sensor is equal to zero ($\overline{Y}_1 = 0$). The domain of solution for the integral equation (25) and the Riccati's equation (27) was specified on the uniform spatial-frequency grid $N_x \times N_\omega$, with $N_x = 21$ and $N_\omega = 101$. The program was written in Fortran77. For simplicity, the upper horizontal vinculum will be omitted below in this paragraph and in Figs. 4–7.

The Fredholm's integral equation (25) of the first kind was solved by means of the Tikhonov's method and by using the standard program TIKH1 from the monograph [16]. In this program only the initial value of the regularization parameter α_T should be specified. After the regularization parameter is selected automatically by the algorithm on each step of the iteration procedure by means of the technique of generalized residuals. In our calculations the initial value of the regularization parameter α_T was specified as:

$$\alpha_T = \varepsilon_R^2; \quad \varepsilon_R = \varepsilon_S(\omega_{\max} - \omega_{\min})^{1/2}, \tag{29}$$

where ε_S is the accuracy of the input admittance measurements and ε_R is the accuracy of the right-hand side of the Eq. (25). In all calculations, the first-order regularization was used.

The Riccati's equation (27) was solved numerically with the use of the BR algorithm [17] (see Appendix A). Integrating the Riccati's equation, we found the exact values of $Y_S(\omega)$, i.e., the right-hand side of the integral equation (25). The measurement noise was simulated with the aid of the random number generator and was added to $Y_S(\omega)$. The measurement noise was generated in accordance with the Gaussian law with zero average value and with the root-mean-square value equal to ε_S.

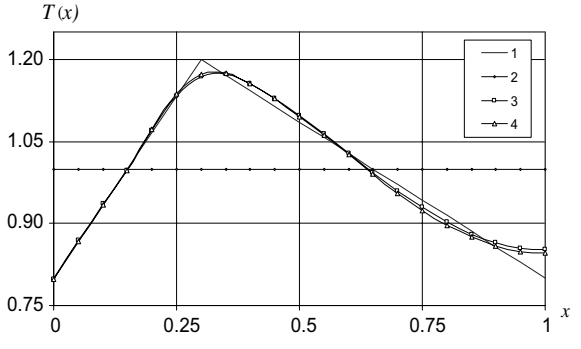

Fig. 4. Restoration of the "triangle" temperature profile from the one end of the sensor. The case of CDS with pure capacitive cross conductivity y_0: 1—unknown temperature profile; 2—initial approximation to temperature profile; 3—restoration profile after two iterations ($n = 2$); 4—final restoration profile (four iterations, $n = 4$).

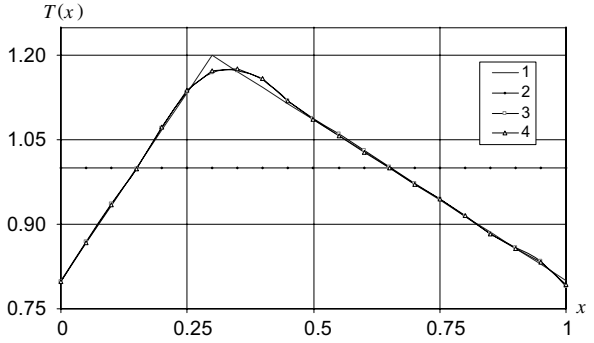

Fig. 5. Restoration of the "triangle" temperature profile from two ends of the sensor. The case of CDS with pure capacitive cross conductivity y_0: 1—unknown temperature profile; 2—initial approximation to temperature profile; 3—restoration profile after two iterations ($n = 2$); 4—final restoration profile (five iterations, $n = 5$).

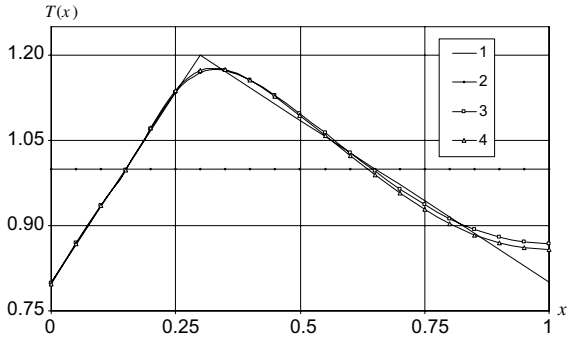

Fig. 6. Restoration of the "triangle" temperature profile from the one end of the sensor. Cross conductivity y_0 takes into account the leakage due to non-ideality of the dielectric material: 1—unknown temperature profile; 2—initial approximation to temperature profile; 3—restoration profile after two iterations ($n = 2$); 4—final restoration profile (five iterations, $n = 5$).

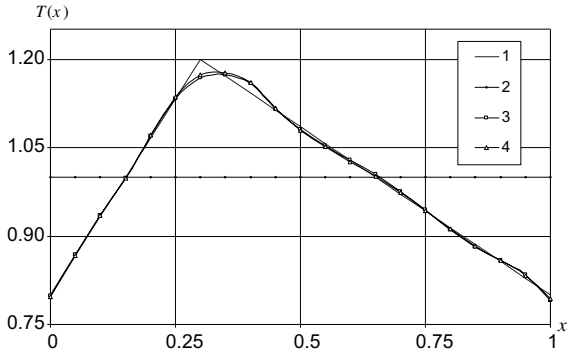

Fig. 7. Restoration of the "triangle" temperature profile from two ends of the sensor. Cross conductivity y_0 takes into account the leakage due to non-ideality of the dielectric material: 1—unknown temperature profile; 2—initial approximation to temperature profile; 3—restoration profile after two iterations ($n = 2$); 4—final restoration profile (five iterations, $n = 5$).

Two types of sounding was used, namely from the one (left) end of CDS and simultaneously from both ends. Sounding from both ends of the sensor allows to improve the accuracy of the method. Indeed, in this case two temperature profiles were obtained $T_1(x)$, $T_2(x)$, as the results of measurements from the left and the right ends of the sensor. The errors of restoration of the temperature profile increase with the distance, so some reasonable "averaging" of the obtained profiles $T_1(x)$, $T_2(x)$ can be useful. In this paper we introduce the resulting profile $T(x)$ by using weight multipliers w_1 and w_2:

$$T(x) = w_1 T_1(x) + w_2 T_2(x), \quad 0 \leqslant x \leqslant 1, \tag{30}$$

where:

$$w_1 = -5(x - 0.6); \quad w_2 = +5(x - 0.4) \text{ at } 0.4 \leqslant x \leqslant 0.6;$$
$$w_1 = 1; \quad w_2 = 0 \text{ at } 0 \leqslant x < 0.4;$$
$$w_1 = 0; \quad w_2 = 1 \text{ at } 0.4 \leqslant x \leqslant 1.$$

6.2. Results of numerical experiments

Numerical simulations of measuring possibilities of CDS were provided for two types of RC structures. From the mathematical point of view the structure of CDS is determined by the cross conductivity y_0 and by the electrical resistance R (see Fig. 3 and Eqs. (1)–(5)). In our simulations we have considered R as a constant.

As for the cross conductivity y_0, we have investigated two cases. At first, we have studied the case of pure capacitive conduction when the cross conductivity is equal $y_0 = pC$. Corresponding results are presented in Figs. 4, 5 and 8. Then cross conductivity of dielectric material (leakage conductivity) has been taken into account. For this case the cross conductivity is given by Eq. (4), the results of numerical simulations are illustrated by Figs. 6 and 7.

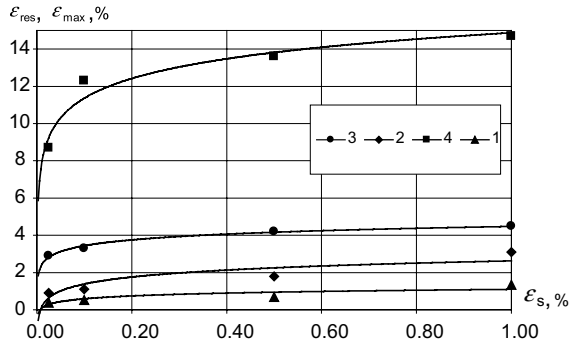

Fig. 8. Errors ε_{res} and ε_{max} of restoration for the "parabolic" temperature profile as a functions of the accuracy of measuring data ε_S. The case of CDS with pure capacitive cross conductivity y_0: 1—mean-square error ε_{res} for the measurements from two ends of the sensor; 2—mean-square error ε_{res} for the measurements from the one end of the sensor; 3—maximum error ε_{max} for the measurements from two ends of the sensor; 4—maximum error ε_{max} for the measurements from the one end of the sensor.

In Figs. 4–7 the results are presented of restoration of the temperature profile which was assigned as a triangle:

$$T(x) = \frac{4}{3}x + \frac{4}{5}, \quad 0 \leqslant x \leqslant 0.3;$$
$$T(x) = -\frac{4}{7}x + \frac{48}{35}, \quad 0.3 < x \leqslant 1.$$

The input data for restoration of the temperature profile $T(x)$ are the frequency characteristic of the input admittance of CDS $Y_S(p_i)$. These data were "measured" with the accuracy of $\varepsilon_S = 0.1\%$ for the frequencies $\omega_i = \omega_{i-1} + \Delta\omega$, where $\Delta\omega = 1/(N_\omega - 1)$, $i = 1, \ldots, N_\omega$, $N_\omega = 101$, $\omega_0 = 0$.

In the Figs. 4 and 6 the results are presented obtained for the case of measurements from the one (left) end of the CDS. In the Figs. 5 and 7 the results are given when the measurements were provided from the both ends of the sensor with fitting of the temperature profile by means of Eq. (30).

Figs. 4 and 6 shown that errors of restoration increase with the increasing of the longitudinal coordinate x and reach the maximum value ε_{max} on the right end of the sensor at $x = 1$ (5.8% and 7.2%). It can be explained by the fact that the length of propagation of the sounding signal is inversely proportional to the square root of the frequency. That is why, for restoration of the temperature profile near the left end of the sensor ($x \to 0$, "near zone") practically all the frequencies ($0 < \omega < 1$) are used. From the other hand, for the restoration of the temperature profile near the right end of the sensor ($x \to 1$, "far-off zone") information is used from the law frequency part of the spectra ($\omega \to 0$), only.

When the measuring are realized from two ends of CDS the errors of the temperature profile restoration decrease more then at twice. In this case the maximal error takes place in the middle of CDS.

Restoration of smooth temperature profiles can be realized with more important accuracy in comparison with that in a form of a triangle. The maximum ε_{max} and the mean-square errors ε_{res} of restoration of the parabolic temperature profile:

$$T(x) = -1.5x^2 + 1.8x + 0.6$$

are presented in Fig. 8 as a function of the mean-square measuring error ε_S.

Our calculations show that the first 2–3 iterations provide very fast convergence of restoration results to an unknown temperature profile. Number of iterations N after which the calculation process is stopped due to the regularization procedure decreasing with increasing of measuring errors ε_S. For example, during restoration of the parabolic profile from one end of the sensor the number of iterations was equal to $N = 10$, 3, 1 for the measuring errors equal to $\varepsilon_S = 0.1\%$, 1%, 2%.

7. Conclusions

Numerical experiments demonstrate real possibilities of constructing CDS on the basis of modern microfilm technologies. One CDS allows to measure temperature profile along its length and is equivalent by its functional possibilities to several tens of conventional temperature sensors. The main advantage of CDS is very limited number of cables (2 or 3) for electrical connection and simplification of measuring electronic devices. Indeed, for one CDS only one measuring channel is needed. As a consequence, the total price of measuring system can be decreased in many times.

Mathematical basis of measuring by means of CDS is the theory and the algorithms of solving ill-posed inverse problems. These algorithms require fast computer calculations combined with automated impedance measurements of high accuracy. Physical realization of CDS is based on the modern microfilm and semiconductor technologies. Without these mathematical and technological components which are in explosive development, is impossible to state and to solve the problems which are discussed in the present paper.

The algorithms proposed in the paper have been used in numerical simulations for restoration of the temperature profile in the presence of measuring noise. The level of measurement noise has been chosen in accordance with possibilities of the modern impedance devices. For law level of the measurement noise (less than 0.1%), the proposed spectral algorithm allows to restore of the temperature field with 1% accuracy. For moderate

level of the measuring noise (0.5–2%), the accuracy of the temperature field restoration becomes about 5–10%. Nevertheless the numerical algorithm remains stable.

Acknowledgements

The authors warmly thank the University of Poitiers and the Ministry of High Education MESRT of France for making this work possible by granting a position of visiting professor to one of them. The work was supported by Russian Fund for Fundamental Research, grant RFFI no. 99-01-0221 and by the French program of pluri-formation of MESRT "Near interface transfer on microscale level".

Appendix A. Algorithm for solving the Riccati's equation

The non-linear Riccati's equation should be solved on the step 3 of the measuring algorithm. Herein we present the method of numerical solution of this equation. There exists a number of algorithms for numeric solution of the Riccati's equation that are based, as a rule, on the iteration procedures. One of such methods makes use of continued fractions [17]. The electric analog of continued fractions are the cascade circuits that are similar to the electrical model of CDS (Fig. 3(b)).

Let k be the ordinal number of a cascade element counted from the left end of the sensor. If we denote the conductivity and the resistance of this cascade element correspondingly as $y_{0k}(x_k, p)$ and R_k, the CDS input impedance can be represented in the form of the following continued fraction

$$Z_S(p) = Z(0,p) = \frac{1}{Y_S(p)} = R_1 + \cfrac{1}{y_{01} + \cfrac{1}{R_2 + \cfrac{1}{y_{02} + \cfrac{1}{R_3 + \frac{1}{y_{03}+\cdots}}}}}. \tag{A.1}$$

In calculations of continued fractions use is made mainly of two basic algorithms: the forward recurrence algorithm (FR algorithm) and the backward recurrence algorithm (BR algorithm) [17]. As is shown in [17], the BR algorithm is more precise as compared with FR algorithm due to smaller number of operations of multiplication and division.

The used of BR algorithm is as follows. We assume that

$$Z_{m+1} = Z_l = 1/Y_l \tag{A.2}$$

and making calculations sequentially from "the tail to the head",

$$Z_k^{(m)} = R_k + 1/(y_{0k} + 1/Z_{k+1}^{(m)}), \quad k = m, m-1, \ldots, 1. \tag{A.3}$$

As the result we obtain

$$Z_S = 1/Y_S = R_1 + Z_1^{(m)}, \tag{A.4}$$

where m is the total number of the cascade elements in CDS electrical model.

References

[1] H. Schaumburg, Sensoren, V3, Teubner, Stuttgart, 1992, pp. 63–80.
[2] Yu.K. Evdokimov, Distributed electrochemical sensor: principles and applications in flow measurements, Sov. Electrochem. 29 (1) (1993) 13–16.
[3] Yu.K. Evdokimov, S.A. Martemyanov, G. Gognet, Spatial structure of hydrodynamical fields in electrolyte flows through steady-state polarography of a distributed electrochemical sensors, Russ. J. Electrochem. 31 (10) (1995) 1197–1199.
[4] Yu.K. Evdokimov, One-dimensional and two-dimensional distributed electrodiffusion sensors for turbulence field measurement, In: C. Deslous, B. Tribollet (Eds.), Proceedings of 3rd Int. Workshop on Electrodiffusion Diagnostics of Flows, Dourdan, France, 1993, pp. 327–340.
[5] V.A. Marchenko, Sturm–Liouville operators and applications, Birkhauser, Basel, Boston, Stuttgart, 1986, pp. 5–60.
[6] J.V. Beck, B. Blackwell, S.R. Clair, Inverse Heat Conduction. Ill-Posed Problems, Wiley, New York, 1985, pp. 11–29.
[7] A.N. Thikhonov, V.J. Arsenin, in: Solutions of Ill-Posed Problems, Wiley, New York, 1977, pp. 8–21.
[8] I.M. Gel'fand, B.M. Levitan, On the defermination of a differential equation from its spectral function, Amer. Math. Soc. Trans. Ser. (2) 1 (1955) 253–304.
[9] W. Rundell, P.E. Sacks, The reconstruction of inverse Sturm–Liouville operators, Inverse Prob. 8 (1992) 457–482.
[10] B. Gopinath, M.M. Sondhi, Transformation of the telegraph equation and synthesis of non-uniform lines, Proc. IEEE 59 (3) (1971) 51–62.
[11] S.K. Li, Wave propagation in non-uniform media with losses, Proc. IEEE 70 (2) (1982) 68–78.
[12] B. Ursin, K.A. Berteussen, Some methods for solving of inverse problems on wave propagation in complex media, Proc. IEEE 74 (3) (1986) 7–10.
[13] Y.M. Chen, A numerical algorithm for remote sensing of the thermal conductivity, J. Comp. Phys. 43 (1981) 315–326.
[14] A.G. Butkovsky, Characteristics of systems with distributed parameters, Handbook, Nauka, Moscow, 1979, pp. 17–20 (in Russian).
[15] A.N. Thikhonov, A.V. Goncharsky, V.V. Stepanov, A.G. Yagola, Numerical Methods for the Solution of Ill-Posed Problems, Kluwer Academic Publishers, Dordrecht, Netherlands, 1995.

[16] A.F. Verlan', V.S. Sizikov, Integral equations: methods, algorithms, programs, Handbook, Naukova dumka, Kiev, 1986, pp. 371–374 (in Russian).

[17] W.B. Jones, W.J. Thron, Continued Fractions: Analytic Theory and Applications, Addison-Wesley, Reading, 1980, pp. 130–141.